

Model of the planar broadband differential waveguide interferometer as a humidity sensor

Kazimierz Gut*

Silesian University of Technology, Department of Optoelectronics, 2 Krzywoustego St., 44-100 Gliwice, Poland

Received May 15, 2020; accepted June 29, 2020; published June 30, 2020

Abstract— The paper presents a model of the planar broadband differential waveguide interferometer. Its response to a change in thickness and refractive index of the waveguide layer due to a change in humidity is presented. The analysis was carried out for the wavelength range from 450 to 850 nm. The orthogonal modes TE₀ and TM₀, which propagate in this wavelength range, are considered. It is shown that by using light near the maximum of the system characteristic, instead of the spectrometer, the total power at the system output can be measured.

Broadband waveguide interferometers open new possibilities for detecting interference signals [1]. The published works present the operation of broadband waveguide interferometers of the equivalents of Mach-Zehnder [2÷4], Young [5] and differential interferometer [6÷7] systems. In this work, the evanescent field of the optical wave is sensitive to waveguide cover changes. A change in the refractive index of the waveguide cover or changes connected with the bond between the ligand and the receptor immobilized on the waveguide surface, cause changes in the phase of the guided modes. Professor Walter Łukosz, who introduced the differential interferometer as a chemical and biochemical sensor, wrote that in microporous waveguides there might be a change in the refractive index n_F of the waveguide layer as a result of absorption or desorption. [8]. The development of nanotechnology and new research capabilities of nanoporous thin layers as optical waveguides are a very attractive research field for sensor techniques [9]. Bio-compatible optical materials have been extensively studied in recent years. In this group of materials, a special attention has been paid to silk *Bombyx mori* (silkworm) silk, known for thousands of years [10÷13]. The waveguide layers obtained from this material have a loss of less than 1dB/cm [11]. When the relative humidity (RH) changes, the thickness and refractive index of the layer change [12]. These changes are reversible. These properties can be used to design a waveguide humidity sensor. The paper presents a model of the broadband differential interferometer which uses changes in the waveguide silk layer to detect changes in the relative humidity of the environment. A three-layer waveguide optical system consisting of a substrate n_S (silicon

dioxide), waveguide layer n_F (silk fibroin) and cover $n_C=1.00$ (air) was considered. This configuration is presented in Fig. 1.

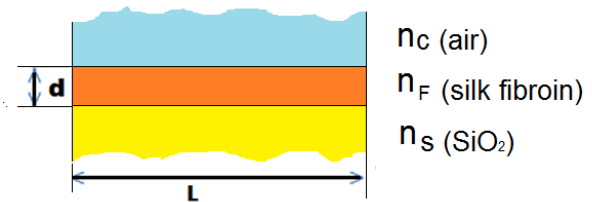


Fig.1. The three-layer system: substrate (SiO₂), waveguide layer (silk fibroin), cover (air).

Based on [13], the dispersion characteristics of the refractive index n_F of the waveguide layer were assumed. The refractive index of the substrate n_S was assumed as in [6].

The values of the effective refractive indices of the orthogonal modes TE and TM were determined as a function of the waveguide thickness d for the wavelength of 450nm and 850nm. The obtained dependencies are shown in Fig. 2.

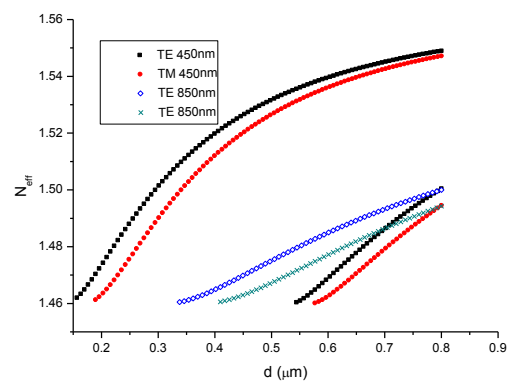


Fig.2. Effective refractive indices as a function of thickness d of the waveguide layer for a wavelength of 450nm and 850nm.

In the case of the waveguide layer of thickness $d = 0.50$ μm , only the fundamental modes TE₀ and TM₀ propagate in the entire range of the spectrum from 0.45 μm to

* E-mail: kazimierz.gut@polsl.pl

0.85 μm . This waveguide thickness was selected for further analysis.

In the differential interferometer, the light from a source of spectral distribution $I_{in}(\lambda)$ after passing through a polarizer causes propagation of the fundamental modes TE_0 and TM_0 . The polarizer at the waveguide output (in front of the detector) reduces the light from both modes to one polarization with a spectral distribution of $I_{out}(\lambda)$.

The intensity of light at the end of the optical path can be expressed by the formula [7]:

$$I_{out}(\lambda) = \frac{1}{2} I_{in}(\lambda) [1 + \cos(\Delta\phi)] \quad (1)$$

where $\Delta\phi$ is the phase difference between the modes of the waveguide. The phase $\Delta\phi$ is a function of the length of the path of propagation L and the difference of the propagation constants [7]:

$$\Delta\phi(l, d, n_F) = [\beta_{\text{TE}_0}(\lambda, d, n_F) - \beta_{\text{TM}_0}(\lambda, d, n_F)]L \quad (2)$$

Then, based on the measurement data presented in [12] [14], the thickness and the dispersion of the refractive index of this layer for a relative humidity of 20%, 40% and 60% were determined. The propagation constants of orthogonal modes ($\beta_{\text{TE}_0}, \beta_{\text{TM}_0}$) and their difference $\Delta\beta = \beta_{\text{TE}_0} - \beta_{\text{TM}_0}$ for different relative humidity were calculated. The determined dependence is presented in Fig. 3. The value of difference propagation constants initially increases, reaches its maximum and then decreases with the growth of the wavelength. If relative humidity increases, the maximum of the curve occurs for the same wavelength (about 0.6 μm) and the maximum value decreases.

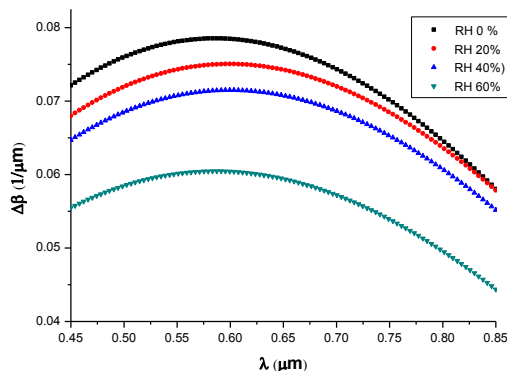


Fig. 3. Dependence of the difference of propagation constants on the wavelength.

Equation (1) can be written as:

$$I_{out}(\lambda) = T(\lambda, L, RH) I_{in}(\lambda) \quad (3)$$

where $T(\lambda, L, RH)$ is the factor that causes a change in the $I_{out}(\lambda)$ spectrum. $T(\lambda, L, RH)$ is the function of propagation path length, wavelength and relative humidity:

$$T(\lambda, L, RH) = \frac{1}{2} + \frac{1}{2} \cos[\Delta\phi(\lambda, L, RH)] \quad (4)$$

Figure 4 shows $T(\lambda, L, RH)$ for 20%, 40% and 60% of relative humidity and for the optical path length $L_1 = 75 \mu\text{m}$, $L_2 = 150 \mu\text{m}$ and $L_3 = 300 \mu\text{m}$.

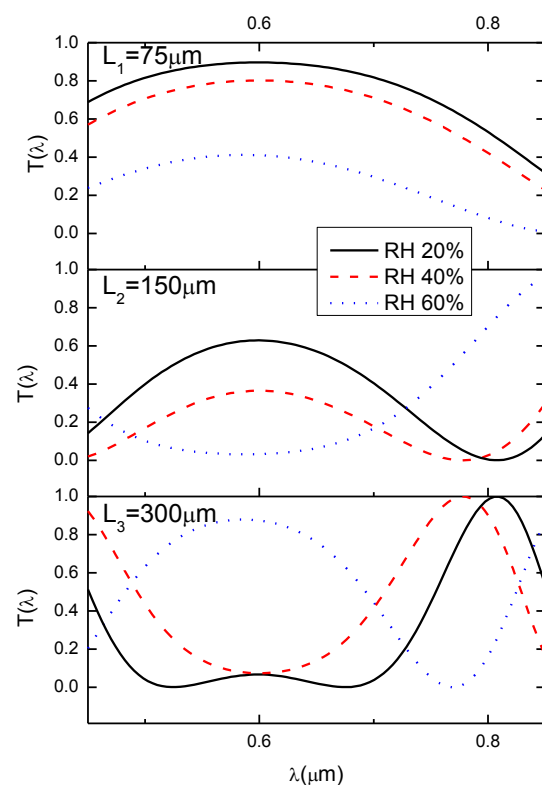


Fig. 4. $T(\lambda, L, RH)$ for 20%, 40% and 60% of relative humidity and for the optical path length L_1, L_2 and L_3 .

The determined characteristics of $T(\lambda, L, RH)$ have slow-changing values around 0.6 μm . If one introduces the light only in a small range around the maximum, you get the same phase difference changes for these wavelengths [7]. The spectrum of a commercial LED [15] was used for the calculations (Fig. 5).

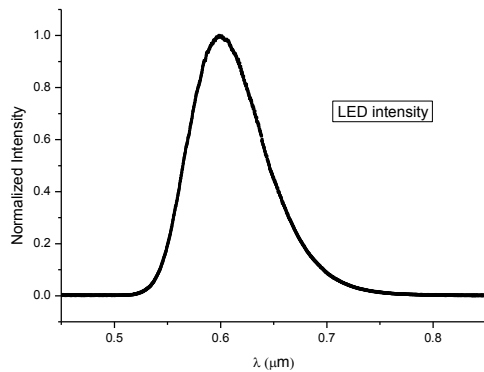


Fig. 5. Light intensity distribution of a commercial LED [15].

The obtained spectral distributions $I_{\text{out}}(\lambda)$ for a relative humidity of 20%, 40% and 60% and for the optical path length L_1 , L_2 and L_3 are shown in Fig. 6.

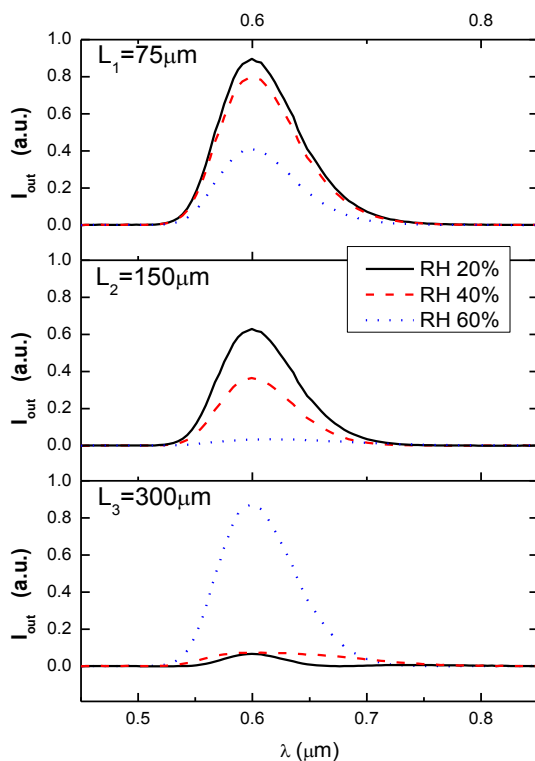


Fig. 6. Distribution of light intensity at the output of the system using LED for 20%, 40% and 60% of relative humidity and for the optical path length L_1 , L_2 and L_3 .

In the broad-band difference interferometer, information about the change of thickness and refractive index of waveguide layers relates to the spectral distribution of the signal transmitted by the system. If one chooses an

appropriate wavelength range at the input of the system (where the characteristic of $\Delta\beta(\lambda)$ reaches its maximum and is relatively flat), the phase difference between the modes will be the same at the output of the system in this range. In this way, instead of recording the spectrum of the signal with a spectrometer, you can record the total output signal with a simple detector.

References

- [1] M. Kitsara, K. Misiakos, I. Raptis, E. Makarona, *Opt. Expr.* **18**, 8193 (2010).
- [2] K. Misiakos *et al.*, *Opt. Expr.* **22**, 8856 (2014).
- [3] K. Misiakos *et al.*, *Opt. Expr.* **22**, 26803 (2014).
- [4] K. Misiakos *et al.*, *ACS Photonics* **6**, 1694 (2019).
- [5] E. Makarona *et al.*, *J. Opt. Soc. Am. B* **34**, 1691 (2017).
- [6] K. Gut, *Opt. Expr.* **25**, 3111 (2017).
- [7] K. Gut, *Nanomaterials* **9**, 729 (2019).
- [8] W. Lukosz, *Sensor Actuat. B-Chem.* **29**, 37 (1995).
- [9] W. Knoll *et al.*, *Analyt. Bioanalytical Chem.* **412**, 3299 (2020).
- [10] A. Bucciarellia *et al.*, *Optical Materials* **78**, 407 (2018).
- [11] V. Prajzler, K. Min, S. Kim, P. Nekvindova, *Materials* **11**, 112 (2018).
- [12] Q. Li *et al.*, *RSC Advances* **7**, 178889 (2017).
- [13] P. Giovanni *et al.*, *App. Phys. Lett.* **111**, 103702 (2017).
- [14] M. Procek *et al.*, *Proc. SPIE* **11204**, 1120409 (2019).
- [15] <https://www.thorlabs.com/thorproduct.cfm?partnumber=M595F2>